Improving the Accuracy of Prediction of Breach Formation through Embankment Dams and Flood Embankments

M. A. A. Mohamed, Dr P. G. Samuels & M. W. Morris
HR Wallingford, Wallingford, UK.

Dr G. S. Ghataora
University of Birmingham, Birmingham, UK.

ABSTRACT: Embankments are constructed for the retention of water for irrigation and supply, and for protecting people, land, and property from flooding. Failure of any embankment poses risks to people and property nearby and the services provided by the embankment. The review of breaching of embankments in this paper identifies significant issues in the parameterisation of the processes in existing models and the data used for calibration. This paper describes the development of a new model the failure of an embankment that can simulate breach formation, and hence consequent risks, more reliably than existing models. The model uses the standard principles of hydraulics, sediment transport and soil mechanics and introduces a new methodology to model the lateral growth of the breach based upon a combination of continuous erosion and mass instability. The model can simulate the failure of different embankments, either homogeneous or composite, by overtopping or piping, and includes a probabilistic distribution for simulating embankment condition and soil parameters. The model has been tested using both experimental and real failure data, with modelling results showing reasonable agreement with observed values for a range of different scenarios.

1 INTRODUCTION

Embankments are constructed for the retention of water for irrigation and supply, and the protection of people, land, and property from flooding. Failure of any embankment poses risks to people and property nearby and the services provided by the embankment. The ability to maintain assets, and provide an acceptable standard of service for water supply and flood defence therefore depends on understanding and predicting performance of the embankments under all conditions. Tools currently available for simulating embankment failure are not very accurate (e.g. Mohamed *et al*, 2001) and can only be used for indicative assessments. Consequently, the prediction of flood risk from embankment breach may be similarly inaccurate. This applies particularly in the critical zone close to the dam or embankment where the risk to life is greatest. Flooding from the failure of the Teton dam in 1976, and from the Mississippi and Missouri rivers, in 1993, and more recently, the Yangtze River in China during1998, are examples of these hazards.

The prediction of potential breaches and the consequent flooding are thus important steps in managing the risk from potential embankment failure. However, breach simulation and breach parameter prediction are considered to contain the greatest uncertainty of all aspects of dam break flood forecasting (Wurbs, 1987, Singh, 1996, and Morris, 2000).

A research project to investigate breach formation through embankments has been undertaken at HR Wallingford, with the following objectives:

1 To review existing methodologies for modelling embankment breaching processes.
2 To identify any weaknesses within these methodologies and determine gaps in current knowledge and understanding.
3 To develop a new methodology that improved the accuracy of prediction of breach formation through embankment dams and flood embankments.

This paper presents an overview of the project giving a summary of weaknesses identified in current methodologies, an overview of a new methodology for predicting breach formation, and an assessment of model performance against a variety of test cases.

2 STATE-OF-THE-ART AND LIMITATIONS

In the last forty years, many models have been developed to simulate the embankment breaching process. In spite of this, the current state-of-the-art for predicting the breaching process still has many uncertainties. A detailed review of existing models

(Mohamed, 2002) has revealed the several weaknesses and gaps within the modelling process, which are discussed in the sections below.

2.1 *Breach Initiation*

Little quantitative information is known about the breach initiation processes for overtopping or piping failure. Determining how the breach initiates will help in reliably determining how long it takes for a breach to develop to a critical point. This in turn can help emergency planners in establishing flood risk and potential warning times for areas downstream of an embankment.

2.2 *Breach Location*

All of the models reviewed (Mohamed, 2002) assumed a breach located centrally within a dam or embankment. However, some failure cases showed that breaching might occur near an abutment rather than in the middle of a dam. Examples include the failures of Teton Dam (Jansen, 1980), Baldwin Hills Dam (Hamilton *et al*, 1971), La-Josefina (Abril, 2001), and the Euclides da Cunha failure (Hughes, 1981). The breach growth and hence outflow from a centrally located breach is likely to be different from a 'side' breach in terms of time to peak discharge, peak value, and hydrograph shape.

2.3 *Data For Calibration and Verification*

Most existing models were calibrated or verified using either or both data sets from the Teton Dam failure or the Huaccoto landslide in Peru. The documented data for these two events is not very detailed. For instance, estimated peak outflow from the Teton Dam failure ranged from 45,000 to 80,000 m^3/s. It was also noticeable that some authors verified their models with data from the piping failure of the Teton Dam in spite of developing their models to only simulate an overtopping failure. Some also calibrated their 'central' breach models (i.e. unrestricted breach growth) with side breach failure data (i.e. erosion was restricted on one side by rock abutments). These wide ranging inconsistencies support the need for good quality data sets (such as large-scale experimental data) for the calibration and verification of breach models.

2.4 *Breach Morphology*

Two common assumptions in many of the existing models are a constant shape (e.g. rectangular, trapezoidal, or parabolic) of the breach and the uniform erosion of the breach section during the formation process. These assumptions simplify the equation(s) used to update the breach section at each time step, but they seem to be physically unrealistic. Assuming uniform erosion throughout the section means that the part of the breach above the water surface will erode at the same rate as that submerged, which is obviously incorrect. It also means that the sides of the breach below the water surface will also erode at the same rate as the breach base, which is inconsistent with the flow stress distribution along the breach sides. Longitudinal growth of the breach was assumed to be parallel to the downstream face in some of the models (BREACH (Fread, 1988), BRES (Vissser, 1998) models). This representation is not compatible with the assumptions of continuity for sediment transport (Mohamed, 2002). For example, the BREACH model computes the flow depth and velocity along the downstream face of the embankment using the steady uniform flow equation. This flow condition, if combined with the sediment continuity equation, will not give parallel retreat of the downstream face.

2.5 *Hydraulics of the Flow over the Embankment*

Most existing breach models use two techniques to simulate flow over the crest and on the downstream face of the embankment. These are:

- the broad crested weir equation and
- the 1-D Saint Venant equations (a simplification)

The Saint Venant equations incorporate the following assumptions (Cunge *et al*, 1980):

- The flow is one-dimensional.
- The water pressure is hydrostatic.
- Boundary friction and turbulence effects can be accounted by steady state flow resistance laws.
- The average channel bed slope is small.

It is clear that the second and fourth assumptions may not be applicable for breaching of embankments. Since the streamline curvature is not small, vertical acceleration may not be negligible. Also, the downstream face of the embankment may be considered as steep in hydraulic terms. In the derivation of the broad crested weir formula, the curvature of the flow is taken into consideration. The weir formula is thus often used to calculate the flow over the crest since it accounts for the acceleration of the flow to the critical point on the crest.

The steady non-uniform flow equations have also been used to compute the water depths, velocities, and energy slope on the downstream slope due to the short reach of the breach channel and its steep slope and their relatively simpler computations compared to the Saint Venant equations.

2.6 *Sediment Transport Equations*

The selection of a sediment transport equation to be used in any mobile bed problem is difficult and is typically based on professional judgement, previous experience, or even personal preference. When con-

sidering the breaching process, the problem becomes even more difficult. Most existing sediment transport equations were derived for steady state subcritical flow conditions, for specific types of sediment, and for a certain range of sediment diameters. These conditions are likely to be violated during the breaching process since conditions are typically unsteady, supercritical flow, and with a wide variety of soil types used for embankment construction. Research in the area of the unsteady non-uniform sediment transport is still in its early stages and more work is required in order to achieve reliable results that could be used for simulation of problems such as breach formation. However, in the absence of any other method to predict the sediment transport, careful selection from the existing sediment transport formulae might be undertaken. On selection of these formulae, the following might be taken into consideration:

- Their applicability to flow on steep slopes and for supercritical flow.
- Their derivation (e.g. based on dam breach experimental data?).

2.7 *Geo-Mechanics of the breach*

In all of the breaching experiments that were reviewed by the authors during this research, instability of the breach sides was observed during the breaching process. Most existing models do not consider this process which means that they neglect a process that is likely to be vital, and thus the calibration and validation of these models must be questioned. The models that consider this process use very simplified assumptions e.g. BREACH (Fread, 1988) and BEED (Singh, 1997). Assuming constant breach shape and uniform erosion of this section also affects the accuracy of the slope stability calculations since lateral erosion will tend to steepen the banks and the breach side slope will get steeper and steeper as water flows through the breach (Osman et al, 1988). This means that the side slope of the breach changes throughout the simulation and hence its shape.

2.8 *Modelling Composite Embankments and Surface Protection Layers:*

Despite that composite embankments represent a significant percentage of real embankments around the world, the majority of existing models were developed to simulate failure of homogeneous embankments. The failure of composite embankments might involve other processes such as core wall instability and mixed sediment transport in addition to the processes encountered with homogeneous embankments. Moreover, many man made embankments have surface protection to prevent erosion of the embankment faces (Singh, 1996). The effect of surface protection was either neglected or oversimplified in many of the existing models (BREACH (Fread, 1988)).

2.9 *Key issues for the research*

It is clear that there are many gaps in our knowledge for reliably predicting breach growth and location and the research has focused on the following issues:

1 A realistic representation of breach development during the breaching process.
2 A more accurate analysis of the breach side slope instability process and the transport of this material after the instability.
3 A methodology to model the failure of composite embankments, including the effect of embankment protection layers on breach development.

3 DESCRIPTION OF A NEW METHODOLOGY FOR BREACH SIMULATION

3.1 *Overtopping of Homogeneous Embankments*

Adjusting the breach shape is a crucial process in any embankment-breach model. Several methods have been used in existing models that simulate breach top width adjustments. A new method is proposed to predict top width adjustment. The process assumes a rectangular initial shape of the breach, as water flows into the breach its shape and side slope will change as shown in Figure 1(B). The bottom width and the breach depth will increase as the water erodes the section sides and bottom. The top width will not change significantly and can be assumed constant until slope instability is encountered.

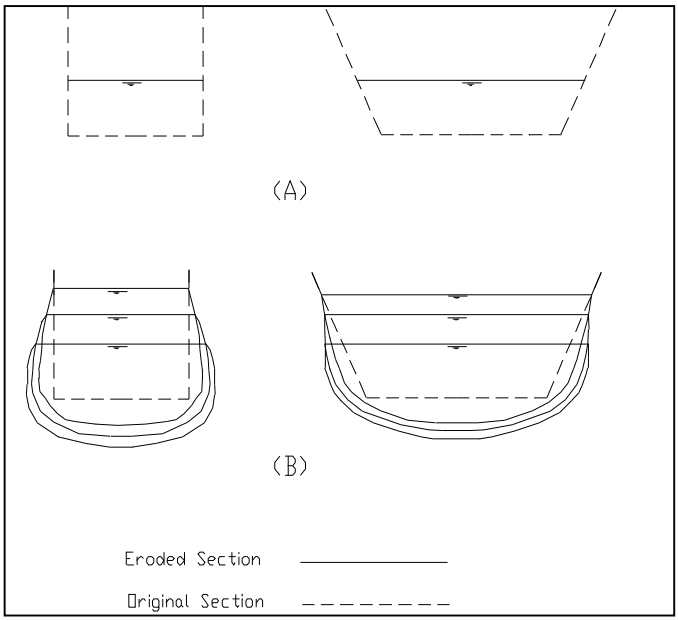

Figure 1: (A) initial breach shape (B) Hypothetical breach shape after three successive time steps.

The process is a combination of continuous erosion and discrete mass failures due to side slope instability. Continuous erosion is calculated by using a sediment transport formula to quantify the volume of the sediment transported. Then by analysing the effective shear stress distribution[1] for the breach section the new breach shape can be obtained, as erosion can be assumed to be proportional to the effective shear stress. The new shape of the breach may be approximated as shown in Figure 2.

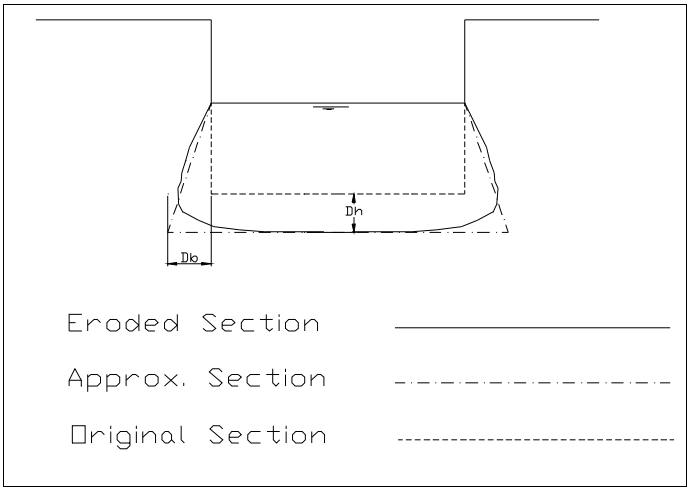

Figure 2: Approximated shape of the breach

The breach section is updated at each time step assuming that maximum lateral erosion (Db) is equal to the vertical erosion (Dh) and it is assumed to occur very near to the bottom level of the breach. The top width is kept constant until slope instability is encountered. The stability of the breach side slope is analysed by taking into consideration the forces acting on the slope, and variation of the soil density. A factor of stability (FOS) is obtained using the following equation:

$$FOS = (\text{Stabilising Forces} / \text{Destabilising Forces}) \quad (1)$$

Where:

The stabilising forces are:

- Water pressure forces in the breach channel.
- Friction forces.
- Cohesion forces (if any).

The destabilising forces are:

- Gravity forces.
- Pore water pressure forces in the embankment.

The nearly vertical sides of the breach (as observed in both lab experiments and real failures) suggest that slope instability failure modes might be either through shear or bending failure (Mohamed, 2002). Both these modes of failure can lead to a near vertical failure plane. In the following two sections, a description of each failure mode is given.

3.1.1 *Bending Failure*

An initial rectangular notch is assumed on the crest and the downstream face of the embankment. Water flows through the initial notch. Flowing water erodes the breach sides below the water surface and the bottom of the notch and undermines the slope. The erosion process continues until slope instability is encountered. A tension crack develops progressively as the actual tension stress exceeds the soil tension strength. The soil block rotates and falls into the flowing water. Water erodes the slumped material and the process continues until the reservoir is depleted or the breach reaches its maximum dimensions. This mode of failure is likely to occur in cohesive embankments.

The following assumptions have been made in developing the analysis below (Figure 3):

- Suction is neglected in the zone above the water level within the embankment. This zone is considered dry.
- Changes in water level inside the embankment during the embankment failure time are small and can be neglected.

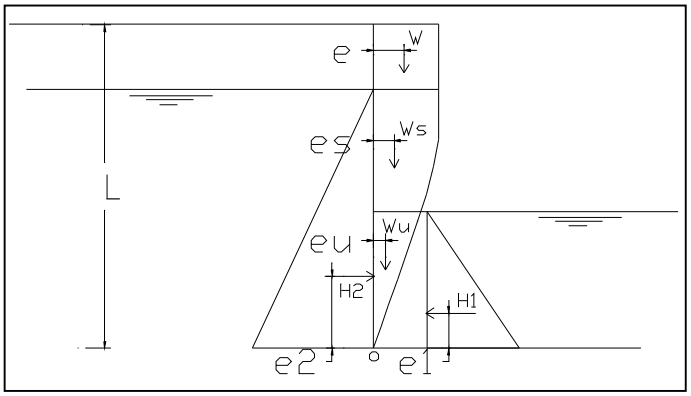

Figure 3: Moments for bending failure

$$\text{Moment}(M_o) = W.e + W_s.e_s + W_u.e_u + H_2.e_2 - H_1.e_1 \quad (2)$$

Where:

W	: Weight of dry block of the soil.
W_s	: Weight of saturated block of the soil.
W_u	: Weight of submerged block of the soil.
H_1	: Hydrostatic pressure force in the breach channel
H_2	: Hydrostatic pressure force inside the embankment.
e, e_s,e_u	: Weight forces eccentricities.
e_1, e_2	: Hydrostatic pressure forces eccentricities.
L	: Length of the failure plane.

1 Effective shear stress equals the difference between the total shear stress and the critical shear stress.

Based on the above analysis, the maximum actual tensile stress ($\sigma_{t(actual)}$) on the plane of failure can be computed as follows:

$$\sigma_{t(actual)} = (H_2 - H_1)/L + 6M_0/L^2 \quad (3)$$

Assuming that the allowable soil tensile strength ($\sigma_{t(soil)}$) is known, then $\sigma_{t(actual)}$ is compared with $\sigma_{t(soil)}$ and if ($\sigma_{t(actual)} > \sigma_{t(soil)}$) then failure occurs.

3.1.2 *Shear Failure*

A similar process to that explained above occurs for this failure mode, however the slope fails due to exceeding the shear strength of the soil (Figure 4). This mode of failure is likely to occur in a non-cohesive embankment.

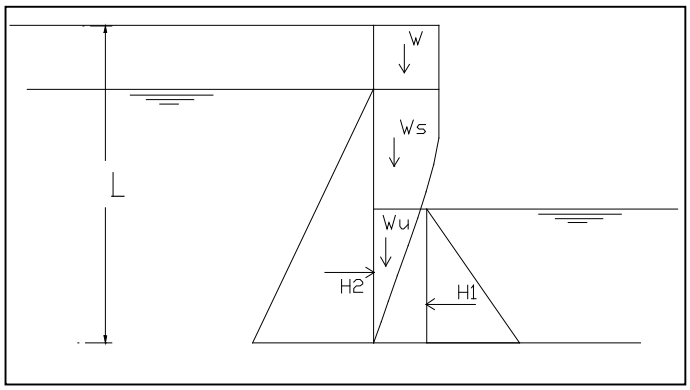

Figure 4: Forces for shear failure.

Making similar assumptions to the bending failure analysis above:

$$FOS = \frac{c * L + H_1 \tan \phi}{W + W_s + W_u + H_2 \tan \phi} \quad (4)$$

Where:

c : Soil cohesion.

ϕ : Soil angle of friction.

3.1.3 *Dealing with uncertainty in soil properties and construction quality*

A probabilistic approach is used to take into account uncertainties in soil properties and the quality of construction. A Sigmoid function has been used to represent a probability distribution for the factor of safety. This was selected since it allows both extremes of 100% and 0% to be represented along with various ranges of distribution in between:

$$f(m) = \frac{1}{1 + e^{a(m-1)}} \quad (5)$$

The value of m represents the factor of safety. The uncertainty coefficient, a, controls the probability distribution and may represent the quality or knowledge of materials within and construction of the embankment (e.g. very good, good or poor material and construction). Three different uncertainty distributions (Figure 5) were used to represent the quality of materials and construction, however, other distributions may also be used to represent varying conditions and uncertainty.

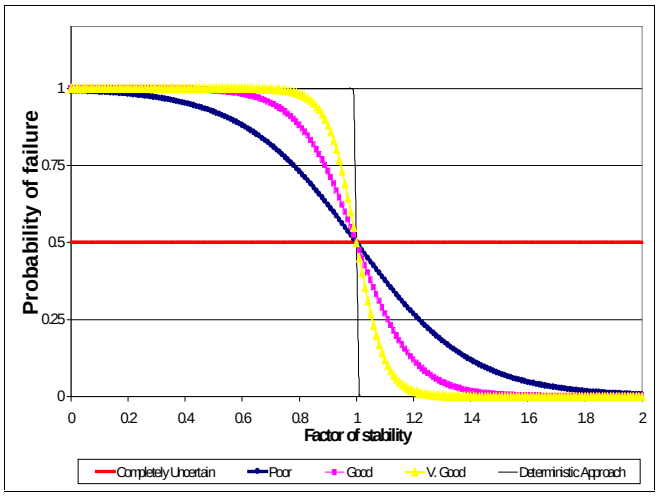

Figure 5: Probability distribution functions for the slope stability factor of safety

3.1.4 *Cohesive Embankments:*

The methodology discussed so far is mainly for non-cohesive embankments with some apparent or conventional cohesion. For cohesive embankments, the failure process might be different. Hughes (1981), Al-Qaser (1991), and Hanson (2000) conducted laboratory and field experiments to determine the failure process of cohesive embankments due to overtopping. They observed the formation of an over fall or steps that progressively advanced towards the upstream face (Figure 6). Hanson (2000) concluded that the erosion process and soil type have a significant effect on the timing and rate of discharge during overtopping events. The observed processes were described as follows:

- Initial downstream surface erosion.
- This initial erosion progresses into stair-stepped multiple over falls.
- Over falls then merge into a single upstream migrating head cut.
- The head cut then migrates upstream, lowering the crest by advancing into the upstream embankment face.

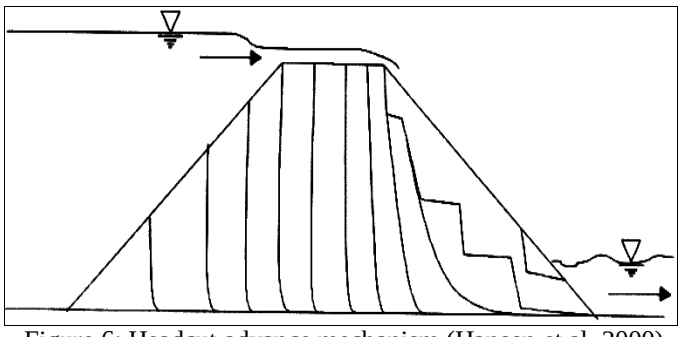

Figure 6: Headcut advance mechanism (Hanson et al, 2000)

Of all the models reviewed within this research, only the SITES model (Wahl, 1998) simulates the

first three processes described above. It does not, however, model the fourth process, which is critical for predicting the flow of water from a breach.

3.2 *Overtopping of Composite Embankments*

The failure of composite embankments differs from that of homogeneous embankments, because of the existence of less erosive layers (such as a clay core) within the dam body. The erosion of the material behind the core may affect the stability of the core and could eventually lead to its failure. The likely failure mechanisms of the core wall of a composite embankment dam, assuming that a large part of the downstream face has been eroded, are:

- Sliding of the clay core wall.
- Overturning of the clay core wall.
- Bending of the core wall.

In the following sections a description of the possible modes of failure of the core are presented.

3.2.1 *Sliding Failure:*

Figure 7 shows the forces acting on the core after a large amount of the downstream body material has been eroded. These forces include:

- Active soil earth pressure forces from the material behind the core (F1).
- Water pressure forces (F2).
- Weight of the clay core material above the failure plane (F3).
- Weight of the material above the upstream face of the clay core and the failure plane (F4).
- Weight of the water above the core (F5).
- Earth pressure forces on the core sides (F6).

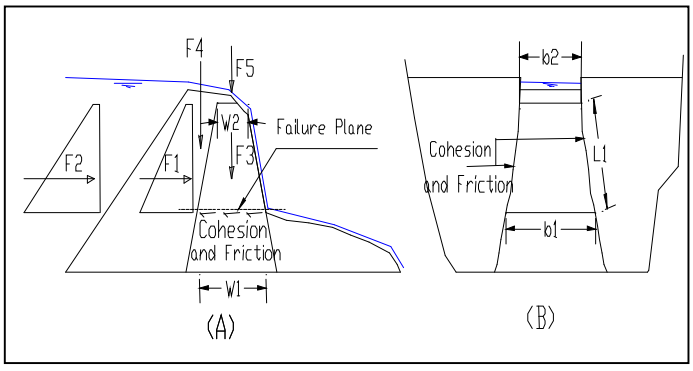

Figure 7: Forces acting on the clay core wall.

The failure plane is assumed to be (as shown in Figure 7) just above the non-eroded material of the downstream face. Forces (F1) and (F2) are the destabilising forces, while the forces (F3), (F4), (F5), and (F6) are stabilising forces. The latter forces mobilise the friction on the bottom and the sides of the failure plane. The cohesion on the right, left, and bottom sides of the failure plane will also resist the destabilising forces. The ratio of the stabilising to the destabilising forces is calculated and if it is less than unity the core is considered to have failed.

3.2.2 *Overturning Failure:*

A similar analysis to that for sliding failure is used here. However, the stabilising and destabilising moments are compared. If the ratio between them is less than unity the core is considered to fail by overturning.

3.2.3 *Bending Failure:*

Hughes (1981) showed that the core failure mechanism could be as shown in Figure 8. He supported this by the observations of Jayasinghe (1978) who noticed similar cracks to those shown in Figure 8 before failure of the core wall.

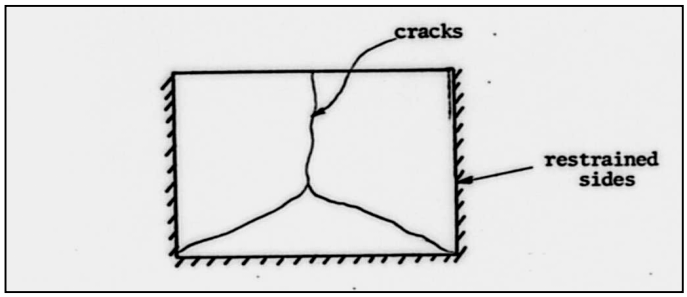

Figure 8: Typical cracking of a clay core restrained on three edges and subject to overtopping (Hughes (1981)).

Analysis of this failure mechanism is difficult because:

1. The geometry of the core and the variation of forces with the height of the core wall.
2. The difficulty in defining the support type on the sides and the bottom of the core wall (hinged, fixed, or something in between).
3. The difficulty in computing the load distribution factors of the core sides and bottom.

The following simplified analysis is proposed for this problem. The clay core might fail by a bending failure as shown in Figure 9 if the left, right, bottom sides can be considered as hinges. Figure 9 (A) shows the failure plane in that case. Figure 9 (B) shows an assumed failure plane neglecting the hinge at the bottom side. This assumption can be justified since the breach depth is likely to be greater than the breach width at that stage of the embankment failure so the effect of the hinge at bottom can be neglected.

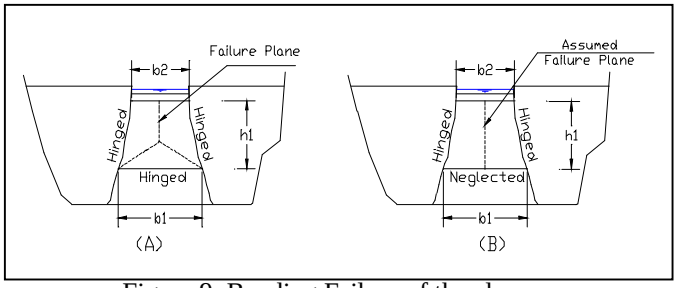

Figure 9: Bending Failure of the clay core

Figure 10 shows the forces acting on the clay core in the case of bending failure after a large part of the downstream face material has been eroded, namely:

– Active earth pressure from the material behind the core (F1).
– Water pressure forces (F2).

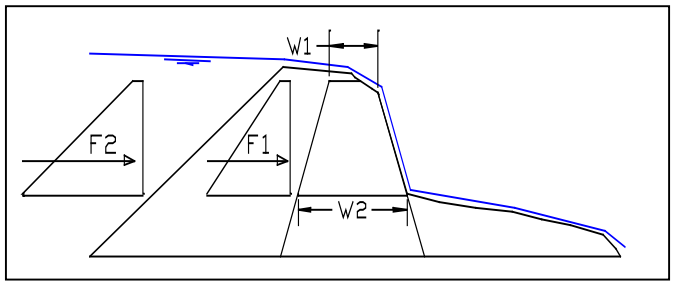

Figure 10: Forces acting on the core wall in bending failure.

The core is assumed to be as a simple beam and the max bending moment and stress is computed. The bending stress can be compared to the tension strength of the clay core material. If the bending stress exceeds the tension strength of the core material then failure will take place.

3.3 *Piping of Embankments*

Piping starts when water flows through an embankment body via cracks, cavities, weak layers etc. As flow increases, the water starts to remove soil particles until a pipe (tunnel) is formed through the body of the embankment (
Figure 11 (A)).

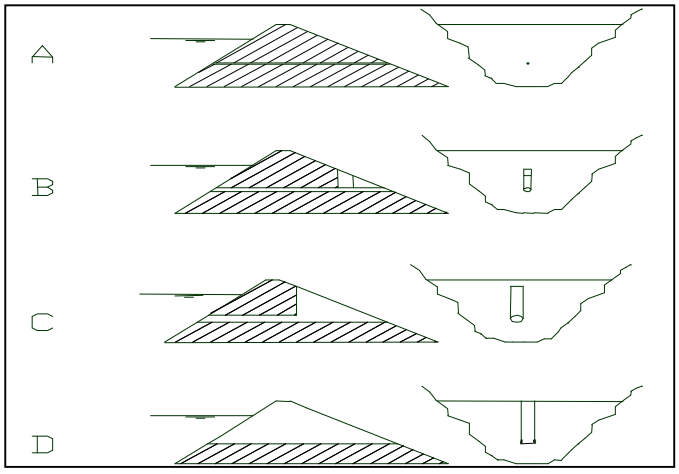

Figure 11: Piping failure in embankments.

After the formation of a pipe inside an embankment, the failure process can be divided into the following processes:
– Erosion of material in the pipe.
– Slumping of the downstream face above the pipe (Figure 11 (B and C)).
– Collapse of the embankment crest, under its own weight or by water pressure Figure 11 ((D)).
– Erosion of the embankment body in a similar manner to that for overtopping breach formation (Sections 3.1 and 3.2).
– In the following sections a description of the modelling procedure for each process is given.

3.3.1 *Erosion of the material in the pipe.*

Figure 12 shows a typical hydrograph for the piping failure of an embankment. It can be noted that different time scales are associated with each process. For the Teton Dam these times were approximately as follows:
– The initiation stage was at least 2 days.
– Erosion of the pipe stage until the collapse of the top of the dam was about 4 hours.
– Emptying of the reservoir was about 2 hours.

The initiation stage was not studied in this research but attention was focussed on growth of an initial pipe.

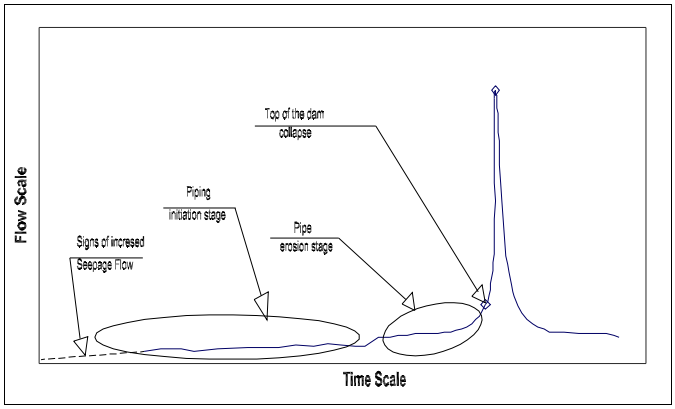

Figure 12: Time scales for piping processes

An initial pipe is assumed to establish within the dam body at the start of the simulation. The flow through the pipe is calculated using the orifice flow equation as follows:

$$Q_b = A\sqrt{2g(H - H_p)/h_L} \qquad (6)$$

Where:
Q_b : Flow through the pipe.
g : Acceleration due to gravity.
A : Pipe cross section area.
H : Water level in the dam.
H_p : Pipe centre line elevation.
h_L : Losses due to friction and contraction.

$$h_L = (0.05 + \frac{fL}{D}) \qquad (7)$$

Where:
f : Friction coefficient determined as function of D_{50}.
L : Pipe Length.
D : Pipe Diameter.

The factor (0.05) in the above equation represents the coefficient of the contraction losses. The enlargement of the pipe was modelled using the simplified procedure used by Fread (1988) and Paquier et al (1998). The pipe is enlarged uniformly along its length based on the volume of sediment eroded

(V_s) within a specified time step. V_s can be computed as shown below:

$$V_s = Q_s \Delta t \quad (8)$$

Where:

Q_s : Sediment transport rate.

Δt : Time step.

It should be noted that this procedure has been used in the absence of any more detailed approaches. This highlights the need for research on the initiation of piping. This simplified procedure can be used for homogeneous and composite embankment dams.

3.3.2 *Slumping of downstream face material above the pipe*

As the pipe develops, material from the downstream face falls into the pipe and is swept away in the flow. This mechanism was observed during the piping failure of the Teton dam in 1976. Justin *et al* (1945) and Hagerty (1991) also reported this process. It is anticipated that the material falls under its own weight. The vertical failure planes observed during the Teton Dam failure and reported by Hagerty (1991) suggest that this is likely to be a shear failure. The ratio between the weight of the material of the wedge and the soil strength is computed. If its value is below unity then the wedge of soil above the top of the pipe is assumed to be unstable.

3.3.3 *The collapse of the top part of the dam, above the pipe.*

As material from the downstream face slumps into the pipe, the width of material above the pipe reduces. If water forces are high enough to exceed the shear strength of the embankment material above the pipe, then this 'wedge' of material may fail. The 'wedge' may also collapse under it is own weight. This mechanism was observed during failure of the Teton Dam. For more information about these failure mechanisms, the reader is referred to Mohamed (2002).

3.3.4 *Erosion of the dam body.*

The process here is similar to that described in Sections 3.1 and 3.2 of this paper, which is a combination of erosion and slumping of material.

4 MODEL PERFORMANCE:

Three sets of data were selected to test different aspects of the proposed new modelling methodology. A detailed description of each case is given in Mohamed (2002) these are briefly summarised below. The test data was obtained from:

– CADAM project Munich proceedings (1998).

– The Teton Dam failure (Fread (1988), and Jansen (1980)).

4.1 *Case 1*

To check the model performance for modelling the overtopping failure of homogeneous embankments, a set of data was used from a series of laboratory experiments that were carried out at the Federal Armed Forces University in Munich (Bechteler et al, 1998) to explore the 3D-development of a dam breach.

Figure 13 shows the results of test case 1. Three simulations have been carried out using different sediment transport equations (Visser (1998), Yang (1979), and Chen and Anderson (1986)). The available measured outflow hydrograph was compared against the corresponding simulation results. For Visser's and Yang's equations, it can be seen that the model results are reasonably in agreement with the measured results in terms of peak outflow value and timing. Chen's sediment transport equation gave poorer results than the other two. The jagged nature of the plots arises from breach growth through bank instability.

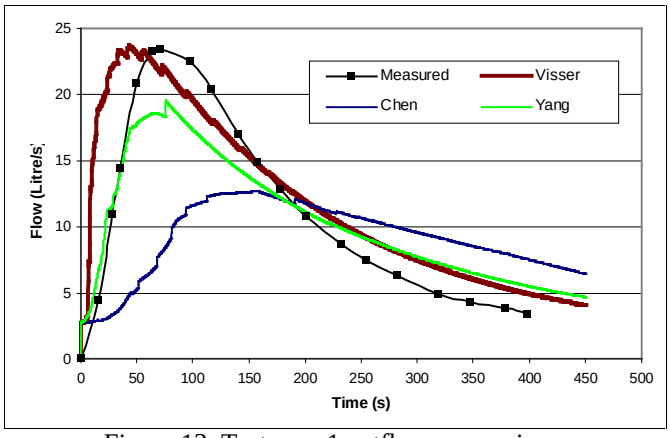

Figure 13: Test case 1 outflow comparison.

Within the CADAM project, several models were tested against the data. A comparison between these models and the developed model is shown in Figure 14 below.

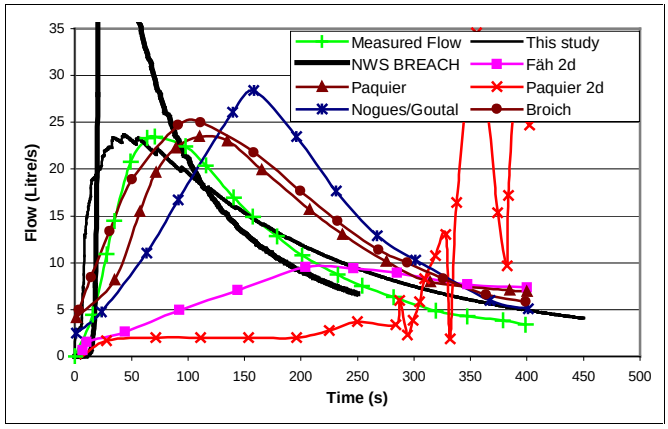

Figure 14: Model comparison (Test case 1).

Apart from the results of Broich's model (which

was calibrated against the test case data) the model performance is generally better than the other models in terms of predicted peak outflow time and value.

4.2 *Case 2*

To check the model performance in modelling the overtopping failure of composite embankments, the data was used from a fuse plug breach test that was conducted in 1982 in the spillway chute of the Yahekou Dam in China. The fuse plug embankment was made of sand fill with a clay core, 5.6 m high and 41 m long at the top and 31 m long at the bottom, with a crest width of 4m, creating a reservoir with a capacity of 46,000 m³.

Two simulations were undertaken using this test case data to investigate the effect of core failure mechanisms. The first considered only sliding and overturning failure modes (A) whilst the second included the bending failure mode (B) as well. This was undertaken to see whether the bending failure mechanism is a critical mode of failure or not, since modelling this failure was based on a simplification of the real processes (See Figure 15).

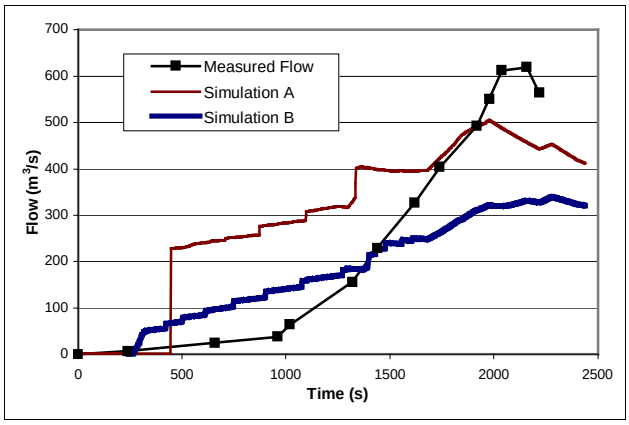

Figure 15: Test case 4 outflow comparison.

The predicted peak flow and its time for simulation A was closer to the measured value than those predicted in simulation B. However, the predicted time of the first failure of the core was earlier than what was observed during the experiment for the two simulations. For simulation A, the magnitude of the flow at the first core failure was significantly higher than the measured value. Whilst, for simulation B, it was slightly higher than the measured value. The results obtained here showed that further investigations and tests are needed to check the performance of the model of the composite embankments.

4.3 *Case 3*

The data of Teton dam failure was used to test the model performance in modelling piping failure of embankments. The Teton dam failed on the 6th of June 1976. The dam was a 91.45 m high earth dam with a 914.5 m crest length, 10.65 m crest width, and 79.85 m depth storing about 307 million m^3 of water at the time of failure (Fread, 1988). Failure occurred close to the right rock abutment, which potentially restricted lateral growth of the breach.

Modelling the piping failure was undertaken assuming a small initial pipe within the dam, and then a central breach or a side breach after the top of the dam collapses. Figure 16 shows the results obtained from both simulations using Yang's equation. It can be seen that the central breach simulation gave a higher peak outflow value than the side breach case. The results of the central and side breach simulations highlight the importance that the breach location and the valley shape might have on the peak outflow value. This also raises questions as to the validity of models (such as BREACH, BEED) which were calibrated using the Teton dam failure data yet only assumed a centrally located breach.

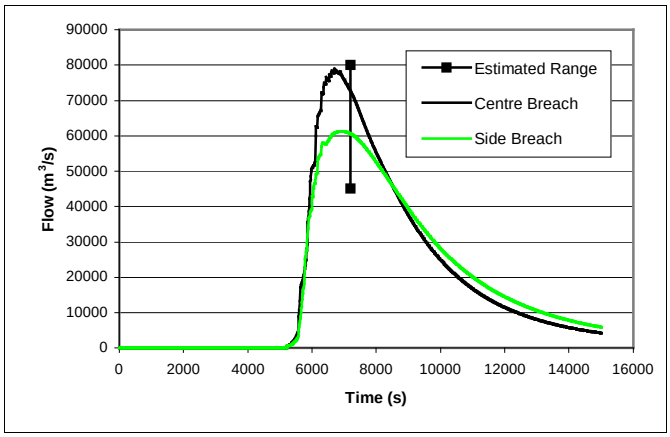

Figure 16: Test case 3 outflow comparison.

To test the effect of using different sediment transport equations on the model results, the Visser, Yang, and Chen and Anderson equations were also used assuming a side breach failure. Figure 17 shows the results obtained using these three equations.

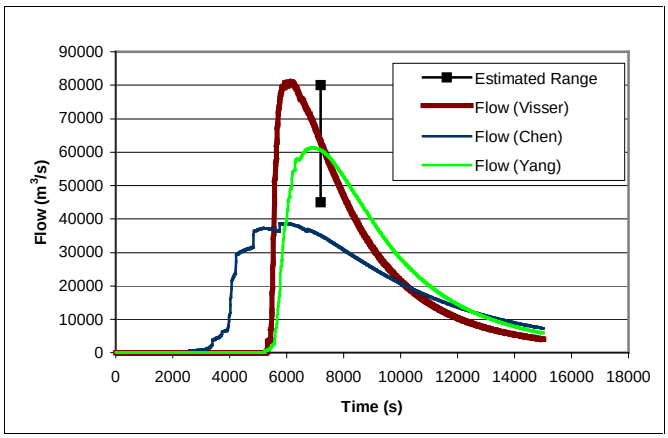

Figure 17: Test case 5 outflow comparison using different sediment equations.

The peak outflow values obtained using Visser and Yang equations were within the estimated range

of the peak outflow value. However the predicted value using Yang's equation was less than that obtained using Visser's equation. The value obtained using Chen and Anderson's equation was below the estimated range. It can also be seen that the time to peak obtained using each equation varied significantly. This variation highlights the importance of selecting a sediment transport equation in dam breach problem and their effect on the results.

5 CONCLUSIONS:

There are several weaknesses in the commonly-used methods for simulating breaching of embankments. These arise from what now appear to be unrealistic simplifications of the breach growth processes and from using as calibration data information from past failures where the valley topography or failure mode were different from those included in the model. Thus the situation is that there remains a high degree of uncertainty on the assessed outflow hydrograph of the water impounded behind an embankment during a failure. This has important social and economic impacts, particularly for risk management and emergency planning.

A new methodology has been put forward in this paper based upon well-established principles of soil and fluid mechanics, although uncertainty still remains in some aspects of the parameterisation of the model. The evidence from the documentation of actual failures is that the failure of an embankment progresses through general erosion of the embankment material and mass failures caused by soil slope instability. The novelties in the model described in this paper includes updating the shape of the eroding part of the breach at each time step rather than assuming a fixed shape and allowing for uncertainty in the knowledge of soil properties through a probabilistic approach. The model has not been calibrated on a particular data set but has been shown to perform well on a range of data obtained from laboratory investigation, field scale measurements and historic failures.

Whilst the model presented here represents and advance on other available methods, several issues remain for further research including:

- the failure processes of embankments with substantial flow parallel to the crest
- the initiation of piping failures
- fracturing mechanisms of exposed clay cores
- the influence of downstream topography on the failure process
- the sediment transport rates for highly unsteady, non-uniform flows, and
- sediment transport for natural mixtures arising from landslide dams.

REFERENCES

Abril, B. 2001. Hipótesis de un Nuevo Deslizamiento del Cerro Tamuga en la Zone de la Josefina Anzlizada Mediante un Modelo Numérico para Rotura de Presas. *1st International symposium on Masses movement*. Cuenca, Ecuador.

Al-Qaser, G. & Ruff, J. F. 1993. Progressive Failure of an Overtopped Embankment. *Hyd. Eng. Proc. of the 1993 National Conf. on Hyd. Eng. San Francisco*. California, USA.

Bechteler, W., & Kulisch, H. , 1998, Description of Test Case No. 1 on Dam Erosion, *Concerted Action on Dam-Break Modelling Proceedings, Munich Meeting*.

Alcrudo, F., Morris, M. & Fabbri, K. 1998, proceedings of the 2nd CADAM workshop, Munich, Germany: Office for official publication of the European Communities.

Chen, Y. H. & Anderson B. A. 1986. Development of a Methodology for Estimating Embankment Damage Due to Flood overtopping. *US Federal Highway Administration Report* No (FHWA/RD-86/126). Fort Collins, Colorado, USA.

Fäh, R., 1996, Erosion-based dambreak simulation, Proc. Of the Second Int. Conference on Hydroinformatics , Zurich.

Fletcher, B. 1992. Center Hill Fuseplug spillway Caney fork River, Tennessee. Hydraulics Laboratory, US Army Crops of Engineers. Technical Report HL-92-15.

Fread, D. L. 1988. *BREACH: an Erosion Model for Earthen Dam Failures. Model description and User Manual*, US National Weather Service.

Hagerty, D. J. 1991. Piping / Sapping Erosion I. Basic Considerations. *Journal of Hyd. Eng.*, Vol. (117), No. (8).

Hamilton, D. H.& Meehan, R. L. 1971. Ground Rupture In The Baldwin Hills. *Science*, Vol. (172), No. (3981), 333-344.

Hanson, G. J. 2000. Preliminary Results of Earthen Embankment Breach Tests. *ASAE Annual international Meeting*, July, Paper No. (002007).

Hughes, A. K. 1981. *The Erosion Resistance of Compacted Clay Fill in Relation to Embankment Overtopping*. Vol.(I) PhD Thesis, The University of Newcastle Upon Tyne.

Jansen, R. B. 1980. *Dams and Public Safety*. The US Department of the Interior, Water and Power Resources Services (Now the Bureau of Reclamation).

Justin, J. D., Hinds, J. & Creager, W. P. 1945. *Engineering for Dams Volume III: Earth, Rock-Fill, Steel, and Timber Dams*. New York.: John Wiley & Sons INC.

Mohamed M. , 2001, Uncertainties in Dam Failure Modelling using the US NWS BREACH model, *Proc. of the Conf. River Basin Management*, Ed Falconer & Blain, WIT press

Mohamed, M. 2002. *Embankment Breach Formation and Modelling Methods*. PhD. Thesis. (To be Published).

Morris, M. W. 2000. CADAM: A European Concerted Action Project on Dam Break Modelling. *Biennial Conference Proceedings, British Dam Society*. Thomas Telford.

Osman, A. M. 1988. River Bank Stability Analysis. I: Theory. *Journal of Hyd. Eng*., Vol. (114), No. (2), 134 -150.

Paquier, A., Nogues, P. & Herledan, R. 1998. Model of Piping in order to Compute Dam-break Wave. *CADAM Proc., Munich Meeting*, Germany.

Singh, V. P. 1996. *Dam Breach Modelling Technology*, Dordrecht, Boston, London.: Kluwer Academic.

Visser, P. J. 1998. Breach Growth in Sand-Dikes. *Communication on Hyd. and Geotech. Eng*., TU Delft, Report no. 98-1.

Wahl, T. L. 1998. *Prediction of Embankment Dam Breach Parameters - Literature Review and Needs Assessment*. U.S. Bureau of Reclamation.

Wurbs, R. A. 1987. Dam-Breach Flood Wave Models. *Journal of Hyd. Eng*., Vol. (113), No. (1), 29-46.

Yang, C. T. 1979. Unit Stream Power Equation for total load. *Journal of Hydrology*, Vol. (40), 123-138.